ACTA UNIVERSITATIS AGRICULTURAE ET SILVICULTURAE MENDELIANAE BRUNENSIS

Volume 67 54 Number 3, 2019

THREE-DIMENSIONS MODELLING OF A JET PILE CONSTRUCTION IN THE KAROLINKA DAM

Somia Bredy[1], Jan Jandora[1]

[1]Brno University of Technology, Faculty of Civil Engineering, Institute of Water Structures, Veveří 95, 602 00 Brno, Czech Republic

To link to this article: https://doi.org/10.11118/actaun201967030637
Received: 10. 9. 2018, Accepted: 15. 4. 2019

To cite this article: BREDY SOMIA, JANDORA JAN. 2019. Three-Dimensions Modelling of a Jet Pile Construction in the Karolinka Dam. *Acta Universitatis Agriculturae et Silviculturae Mendelianae Brunensis*, 67(3): 637–648.

Abstract

Karolinka Earth Fill dam was built on the Stanovnice river above the town of Karolinka in the region of Vsetín. Because of leakage on the downstream dam face due to bad compacting of soil during the construction stage, the reservoir was used to a limited level. There were some steps to improve safety which had been developed to reconstruct the dam after extensive surveys in 2005. The major rehabilitation was commenced in period from September 2012 till October 2013, included the remediation of central impervious core in the dam by using the diaphragm wall (I also have worked on) and jet grouting pile from self-hardening cement-bentonite suspension. The article presents three-dimensional modelling of a jet pile construction, by using finite element method which is performed by Plaxis program. It is concluded that real data shows good agreement with the computed result obtained by the FEM analysis.

Keywords: Karolinka dam, jet grouting, Plaxis 3D, water head, displacement, autogenous shrinkage

INTRODUCTION

The grouting technology has been used for more than two centuries, as an essential factor and an engineering method in order to avoid disastrous accidents and achieve the required advantages. Jet grouting is a most popular method of ground improvement. This technique is widely used over the world. Its application has been grown to large variety of purposes as reducing structure displacements, increasing the bearing capacity and supporting open underground excavation. It is cutting and mixing the soil with grout material under high speed to form cylindrical columns (Fang *et al.* 1994) The first applied of jet grouting to the soil was in 1965 by Yamakado brothers, under the name (the chemical churning pile (CCP) method (Xanthakos *et al.*, 1994). In the early 1970s Japanese Engineers T. Yahiro and H. Yoshida developed jet grout (JG) method (Xanthakos *et al.* 1994). There are three jet grouting systems depending on the number of fluids injected into the subsoil: single tube (grout), double tube (grout + air), triple tube (grout + air + water). At present jet grouting method is applied in a number of engineering construction (tunnel, dam, foundation, excavation support, etc..). Jet grouting technique is used in earthen dam for reducing seepage through its body and foundation, without disturbing the nearby existing structures or lowering water level in the reservoir. Much research has been carried out on the behaviour of jet pile induced in soil dam. Nikbakhtan and

others investigated of the jet grouting effect on slope stability at Shahriar dam by using 3D analysis with Clara-W program (Nikbakhtan *et al.* 2007). Croce and Modoni presented the design of jet-grouting piles for various dam types, with particular attention to the discontinuities along the jet piles because of treatment axes deflection and difference of the jet-column's diameter (Croce *et al.* 2007). Michael and others presented a studied case of the jet grout columns construction to reduce seepage in the spillway and foundation of Morrison Dam (Michael *et al.* 2015). This study deals with design of jet grouting pile for Karolinka dam by the Finite Element Method (FEM).

MATERIALS AND METHODS

Formulation of problems

Variables

The three dimensional problem (3D) of stress-strain and displacement depend on these variables

- Six Components of Stress

$$\{\sigma\} = (\sigma_x, \sigma_y, \sigma_z, \tau_{xy}, \tau_{yz}, \tau_{zx})^T \quad (1)$$

- Six Components of strain

$$\{\varepsilon\} = (\varepsilon_x, \varepsilon_y, \varepsilon_z, \gamma_{xy}, \gamma_{yz}, \gamma_{zx})^T \quad (2)$$

- Three components of displacement

$$\{\vec{U}\} = (u, v, w)^T \quad (3)$$

- The pore water pressure

$$\{p_w\} = p_w \quad (4)$$

Boundary conditions

There are two types of boundary conditions in hydrodynamic analyses of dams:

i) Dirichlet Conditions (specified head boundary) Consist in specifying the known value of the variables, usually represents a body of surface water.
ii) Neumann Conditions (specified flow boundary) Consist in imposing the value of the derivative, which are water level gradient boundaries

The Fig. 1 shows the boundary condition of case study (Karolinka dam). The prescribed displacement at borders $\Gamma_{2,3,4}$ assumed to be zero:

$$U|\Gamma_{2,3,4} = 0 \quad (5)$$

The value of water head at borders $\Gamma_{1,5,6,7}$ assumed to be:

$$h|\Gamma_1 = H_1(t) \quad (6)$$

$$h|\Gamma_{5,6} = H_2(t) \quad (7)$$

$$h|\Gamma_7 = Z(x, y, t) \quad (8)$$

Where $H_1(t)$, $H_2(t)$ are known piezometric heads in borders Γ_1, $\Gamma_{5,6}$ respectively and $Z(x, y, t)$ is the free surface water in studied boundary.

The Neumann boundary condition for flow:

$$\left(k_{ij}\frac{\partial h}{\partial x_i}\right)n_i|\Gamma_{2,4} = q_n \quad (9)$$

$$\left(k_{ij}\frac{\partial h}{\partial x_i}\right)n_i|\Gamma_3 = 0 \quad (10)$$

$$\left(k_{ij}\frac{\partial h}{\partial x_i}\right)n_i|\Gamma_7 = 0 \quad (11)$$

Where n_i is normal vector in directions, y, z, q_n is specified seepage in the studied boundary, and h is hydraulic head.

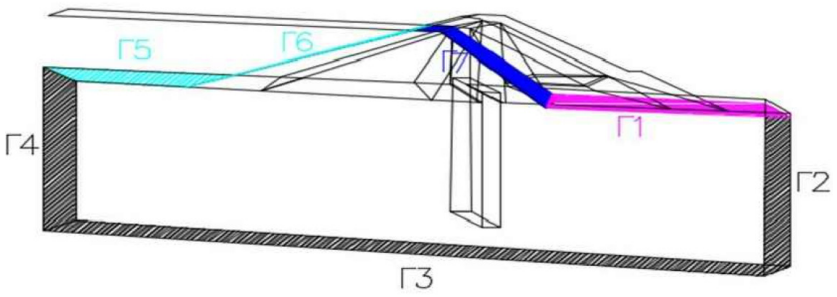

1: *Boundary condition of case study*

Initial conditions

- Initial Displacements
  The hydrodynamic analyses of dams assume at time t = 0, the dam is in the state of static equilibrium and the initial value of the displacements equal zero.
- Initial Ground Water Surface

$$h_{p,0} = H_0 \tag{12}$$

Where $h_{p,0}$ is initial piezometric head in the domain (steady state flow), and H_0 is specified piezometric head.

- Initial Stresses
  The initial stress field is generated by means of the K'_0 procedure using the given (default) K'_0 value in the sub-soil.

$$\sigma'_v = \gamma . d \tag{13}$$

$$\sigma'_h = \sigma'_v . K'_0 \tag{14}$$

Where σ'_v is the vertical effective stress, σ'_h is the horizontal effective stress, and K'_0 is the coefficient for lateral earth pressure (Brinkgreve *et al.*, 2017).

Mathematical modelling

- Displacement State
  The three – dimensional state of stress-strain and deformations is defined as:
  a) Three Static Equations (Cauchy Equations):

$$\left(\frac{\partial \sigma_x}{\partial_x}\right) + \left(\frac{\partial \tau_{xy}}{\partial_y}\right) + \left(\frac{\partial \tau_{xz}}{\partial_z}\right) + F_X = 0 \tag{15}$$

$$\left(\frac{\partial \tau_{xy}}{\partial_x}\right) + \left(\frac{\partial \sigma_y}{\partial_y}\right) + \left(\frac{\partial \tau_{yz}}{\partial_z}\right) + F_Y = 0 \tag{16}$$

$$\left(\frac{\partial \tau_{zy}}{\partial_x}\right) + \left(\frac{\partial \tau_{yz}}{\partial_y}\right) + \left(\frac{\partial \sigma_z}{\partial_z}\right) + F_Z = 0 \tag{17}$$

Where F_x, F_y, F_z denote the body forces per unit volume in *x, y, z* directions respectively.
b) Six Physics Equations (Hook Equations):

$$\varepsilon_x = \frac{1}{E}\left(\sigma_x - \nu\left(\sigma_y + \sigma_z\right)\right) \qquad \gamma_{xy} = \frac{\tau_{xy}}{G} \tag{18}$$

$$\varepsilon_y = \frac{1}{E}\left(\sigma_y - \nu\left(\sigma_z + \sigma_x\right)\right) \qquad \gamma_{yz} = \frac{\tau_{yz}}{G} \tag{19}$$

$$\varepsilon_z = \frac{1}{E}\left(\sigma_z - \nu\left(\sigma_x + \sigma_y\right)\right) \qquad \gamma_{zx} = \frac{\tau_{zx}}{G} \tag{20}$$

- Seepage State
  The analysis of seepage through porous media is implemented in two cases:
  I) Steady state flow analysis

$$\frac{\partial}{\partial x}\left(k_x \frac{\partial h}{\partial x}\right) + \frac{\partial}{\partial y}\left(k_y \frac{\partial h}{\partial y}\right) + \frac{\partial}{\partial z}\left(k_z \frac{\partial h}{\partial z}\right) = 0 \tag{21}$$

  II) Transient seepage analysis
  The three-dimensional governing partial differential equation for seepage through a heterogeneous, anisotropic, saturated unsaturated soil:

$$\frac{\partial}{\partial x}\left(k_x \frac{\partial h}{\partial y}\right) + \frac{\partial}{\partial y}\left(k_y \frac{\partial h}{\partial y}\right) + \frac{\partial}{\partial z}\left(k_z \frac{\partial h}{\partial y}\right) = m\gamma \frac{\partial h}{\partial t} \tag{22}$$

Where k_x, k_y and k_z are coefficient of permeability of soil in *x, y, z* directions respectively, and m water storage.

Numerical Solutions

The numerical technique used in this study is the finite element method (FEM) that was performed by the program Plaxis.

Case study

Karolinka dam was constructed between 1977 and 1984, to supply the cities of Vsetín and Vlara with pure and wholesome water, protect from floods, and generate hydroelectric energy. The first filling of reservoir of Karolinka dam was in year of 1986. Karolinka dam is earth-fill dam made of local gravel materials with a vertical clay gravelly core surrounded from both sides by filters of gravel, the zones of face are formed by gravel sand and The upstream face is reinforced with macadam filled with bitumen. 39.1 meters high, 392 meters long, 1 : 2.2–2.4 downstream slope, 1 : 3.3 upstream slope with reservoir volume of 7.521 million cubic meters and basin area of 23.1 square kilometres. The diameter of a jet pile is (1 m) (Hodák, 2014).

Numerical modelling

The dam, foundation and jet piles were modelled with PLAXIS 3D software in the section Fig. 2. Due to sensitivity analysis, some of parameters

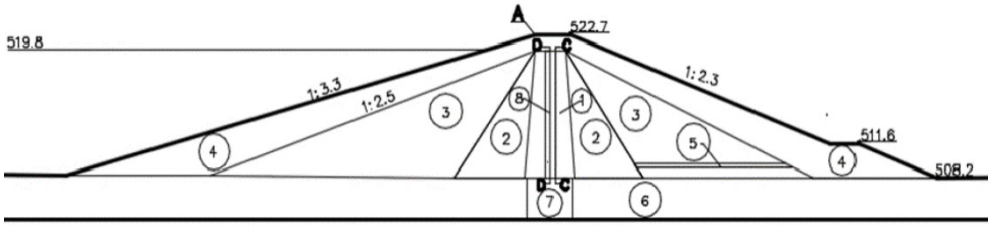

2: *Cross section of Karolinka dam*
1. Core Clay gravelly, 2. Zone 2B Gravel with fine –grained soil, 3. Zone 2A Gravel with loam, 4 Zone 3 Gravel with fine-grained soil, 5. Gravel Drain, 6. Gravel with loam, 7. Curtain Grouting, 8. Jet Pile.

are assumed according to the specifications of the materials in dam. The materials parameters used in modelling is shown in Tab. I.

Mesh Generation and Boundary Conditions

In this modelling, 10-node tetrahedral elements for soil elements were used (Fig. 3). The fine mesh generation of PLAXIS 3D. The domain is discretised into a mesh by 32076 elements through placement of nodal points 52380. With respect to boundary condition in Plaxis 3D, the top (Z_{max}) boundaries set to free and the bottom (Z_{min}) is set to fixed, whereas the right (X_{max}), left (X_{min}), and boundaries: (Y_{min} ,Y_{max}) are set to normally fixed as well. In the ground water flow boundary set boundaries: ($Y_{min,\ max}$), and (Z_{min}) to Closed. The remaining boundaries should be open.

Modelling of soil behaviour

All soils have been modelled as simple linear elastic, perfectly plastic isotropic materials with a Mohr-Coulomb failure criterion. It involves five input parameters, those are E and ν for soil elasticity, the friction angle φ and the cohesion c for soil plasticity, and the angle of dilatncy ψ. Mohr-Coulomb model is a first-order to provide with a reliable result of soil behaviour (Brinkgreve *et al.*, 2017).

Modelling of Pore water pressure changes with time

A fully coupled flow-deformation analysis is conducted to analyses the development of deformation and pore water pressure as a result of time-dependent hydraulic boundary condition (Galavi, 2010).

Modelling jet pile shrinkage

The shrinkage expresses a time-dependent deformation which reduces the volume of element in all directions during the hardening process of the element due to water loss. Mineral admixtures such as fly ash is added as cementing materials, also has a clear effect by enhancing the pore refinement of the cement paste, and increasing in capillary tension, which leads to more shrinkage.

I: *Material properties*

Parameters	Core	Zone 2b	Zone 2a	Zone 3	Sub Soil	Jet pile	Mixture	Curtain	Drain	Bentonite
Hydraulic conductivity [m/day]	0.086	0.864	0.864	4.320	4.320	$0.864.10^{-3}$	$0.864.10^{-4}$	/	86.4	$0.864.10^{-5}$
Unsaturated Unit weight [kN/m³]	19	19	19	19	19	12.5	12.5	25	20	10.5
Saturated Unit weight [*kN/m³*]	21	21	21	21	21	12.5	12.5	25	21	10.5
Young's modulus [kN/m²]	20.10^3	70.10^3	70.10^3	70.10^3	70.10^3	25.10^3	500	40.10^6	100.10^3	400
Poisson's ratio [-]	0.3	0.2	0.2	0.2	0.2	0.25	0.4	0.1	0.15	0.4
Cohesion [kN/m²]	21	1	1	1	1	200	18	/	1	16
Friction angle [°]	/	33	33	33	33	/	/	/	37	/

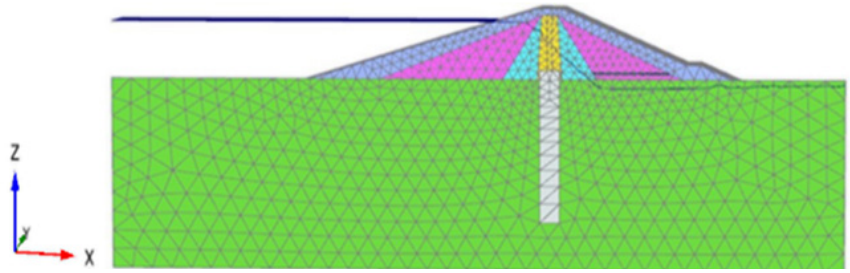

3: *Generated mesh*

The autogenous shrinkage is the change in volume due to the chemical process of hydration of cement (0.4 cm^3/100 gr cement) (Tazawa, 1997). It was modelled by applying a contract surface to the jet pile in hardened state after calculating the value of the shrinkage depending on the typical mix proportions of the pile, the ratio and the mass of cement in mixture.

Modelling of pile-soil interaction

The interaction between the structural element and the soil is modelled by means of the interface. It is used to reduce the friction between the pile and the soil. It is termed as $R_{inter,}$ and its value ranges between 0.01 and 1. Depending on some recommendations (Schweiger *et al.* 2012) the interface elements in our case study are presented between the pile and the core with the value of 0.75.

Modelling of impact loading

The loading included:
- Weight of machine
- Angular moment of jet rod M
- Lifting force F
- Feed force N
- Rotation torque Mn

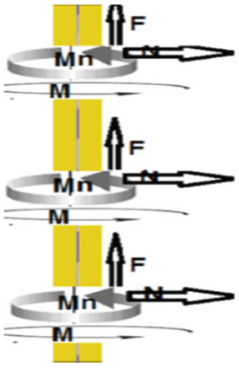

4: *Drilling rod*

Investigation of the failure state

The Mohr-Coulomb failure criterion can be written as the equation for the line that represents the failure envelope (Labuz, Zang, 2012)

$$\tau_f = \sigma'_N \tan\varphi' + \acute{c} \tag{23}$$

Where τ_f is shear stress, σ'_N is effective normal stress, φ' is effective angle of internal friction and $\acute{c}$ is effective cohesion.

From the geometry of Mohr circle:

$$\sin\varphi' = \frac{R}{c'\cot\varphi' + P} = \frac{\sigma'_1 - \sigma'_3}{c'\cot\varphi' + \frac{\sigma'_1 - \sigma'_3}{2}} \tag{24}$$

$$\frac{\sigma'_1 - \sigma'_3}{2} = \sin\varphi' \frac{\sigma'_1 - \sigma'_3}{2} + c'\cos\varphi' \tag{25}$$

$$\sigma'_1 - \sigma'_3 = \sin\varphi'(\sigma'_1 + \sigma'_3) + 2\acute{c}\,\mathrm{con}\varphi' \tag{26}$$

$$\sigma'_1 = \sigma'_3\left(\frac{1+\sin\varphi'}{1-\sin\varphi'}\right) + 2\left(\frac{\cos\varphi'}{1-\sin\varphi'}\right) \tag{27}$$

So the failure criterion can be expressed in terms of the relationship between the principal stresses:

$$\sigma'_1 - \sigma'_3 = \tan^2\left(\frac{\varphi'}{2} + 45\right) + 2\acute{c}\tan\left(\frac{\varphi'}{2} + 45\right) \tag{28}$$

Where σ'_1, σ'_3 are major and minor effective principal stress respectively.

Jet grouting procedure

Fig. 6, shows the construction sequence modelling. The modelling procedures are summarized as follows:

i) Decrease water level 10 meters in 10 days duration.
ii) Add weight of drilling machine.

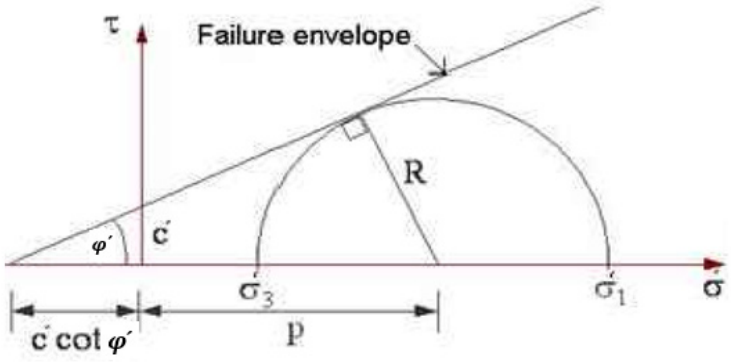

5: *Mohr diagram and failure envelope*

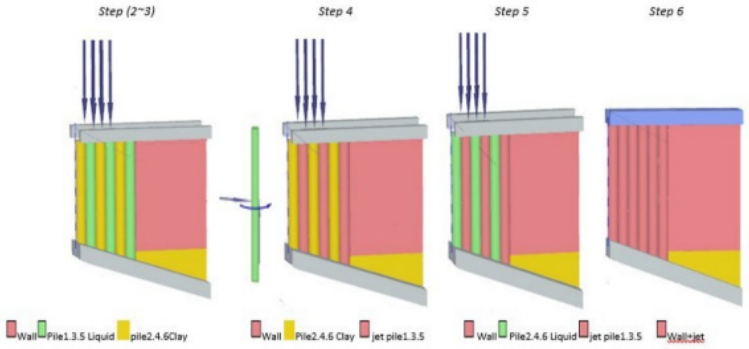

6: *Construction sequence for jet pile*

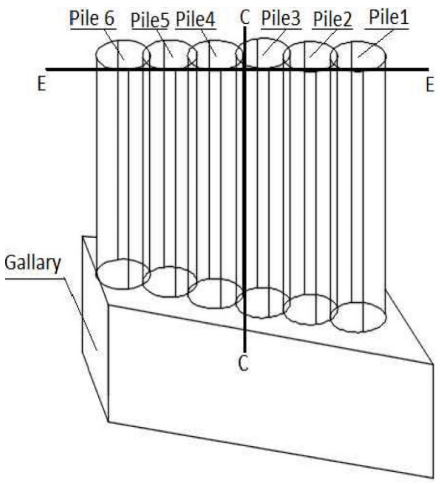

7: *Cross-Section lines*

iii) Build jet piles (1, 3, 5) as volume cylinder with adding interfaces and moment and forces in liquid state.
iv) Cure liquid mixture by applying harden mixture.
v) Apply the same modelling procedures to piles (2, 4, 6).
vi) Increase water level 10 meters in 15 days duration.

RESULTS AND DISCUSSION

The result of the finite element analysis is depicted in Figs. 8~14, Figs. 8–9, show the variation of ground water head during decrease and increase water respectively.

Displacement result are expressed in the figures. 10~13 Fig. 10, shows the horizontal displacement distribution with depth at line cross section C–C (see

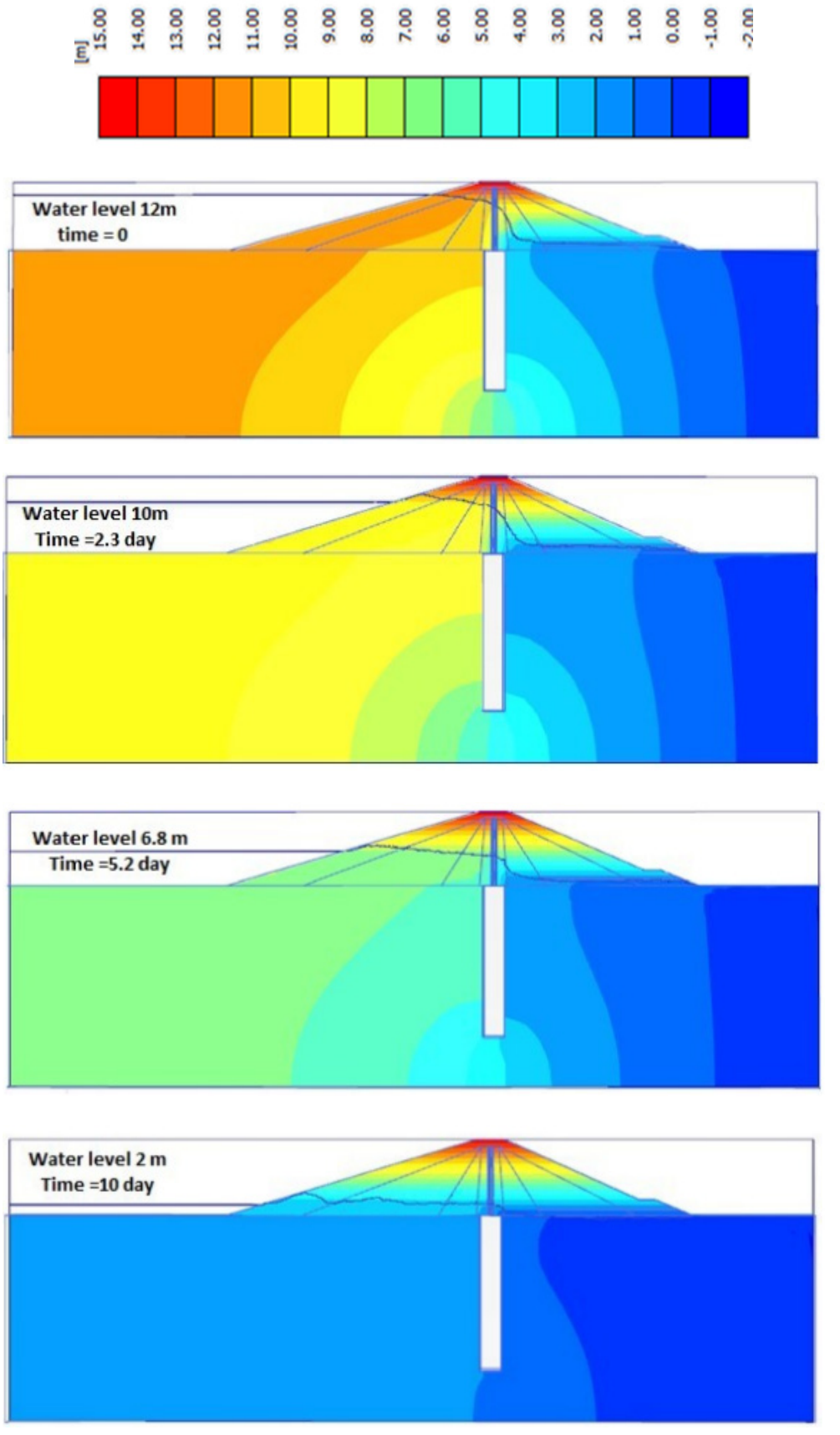

8: *Variation of ground water head (decrease water level)*

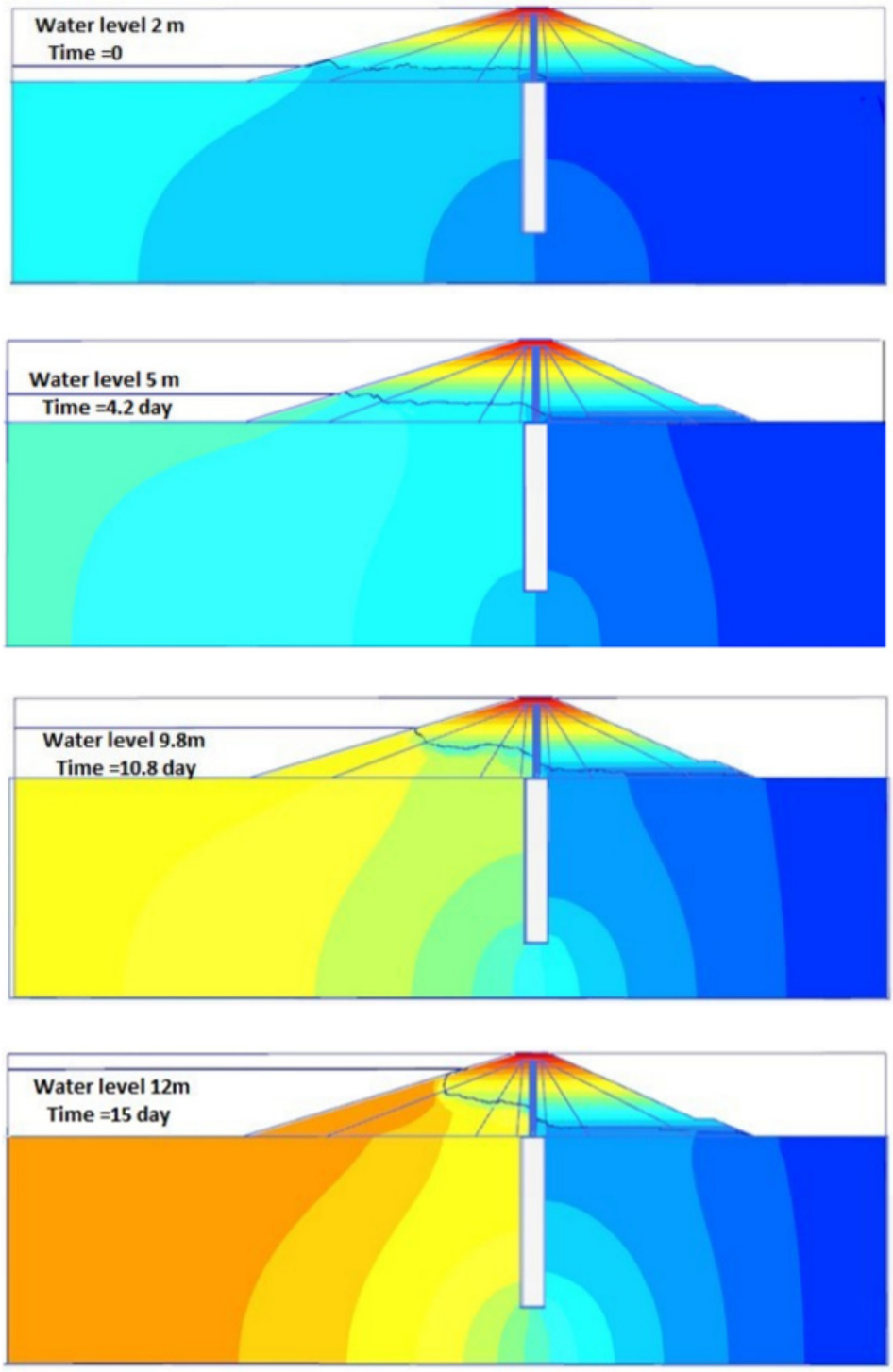

9: *Variation of ground water head (increase water level)*

Fig. 7). It is clear that maximum value of horizontal displacement reached 17.5 mm during decrease water level in reservoir. On the other hand, there is no significant horizontal displacement in the last state. Figs. 11–12, show the horizontal and vertical displacement with section length E–E (see Fig. 7) during construction pile (1, 3, 5). Figure. 13, shows the variation of total displacement with loading time associated with machine weight at dam crest. Fig. 14, shows the status of principal stresses for all points considered in the connection zone at line cross section C–C (see Fig. 7). Mohr-Coulomb failure envelope is drawn for core (clay). Regarding this figure, minor principal stress is compressive in

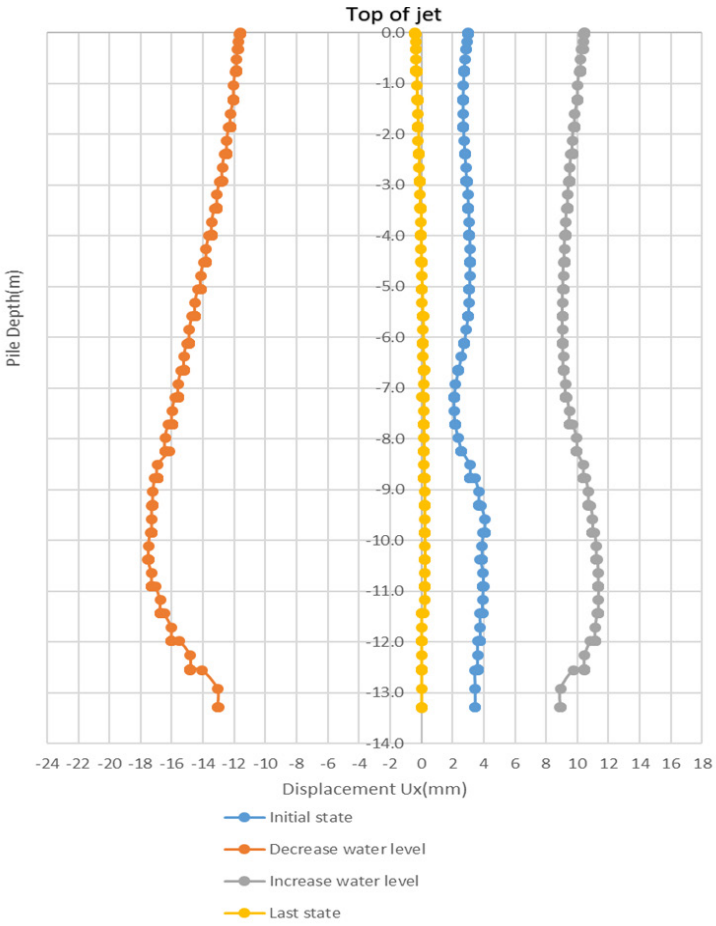

10: *The horizontal displacement along the line cross section C–C (construction pile1, 3, 5)*

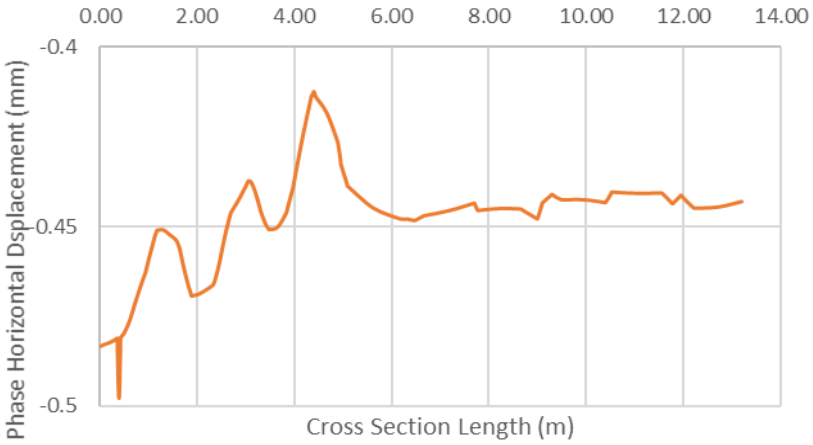

11: *Horizontal displacement at crest dam along the line cross section E-E* (construction jet pile 1, 3, 5)

all connection zone, so no probability of hydraulic fracture occurrence in the connection zone. In other words, the failure of the core does not occur for the connection system.

The prediction in this study for the vertical displacement due to impact loading of drilling-machine was (0.24 mm). The horizontal and vertical displacement during the piles construction almost equal zero, and are agreed with real data in the field measurement performed by TBD company (Hodák, 2014), The results confirm that the analysis was performed for the reconstruction and transient flow as the stages of this analysis.

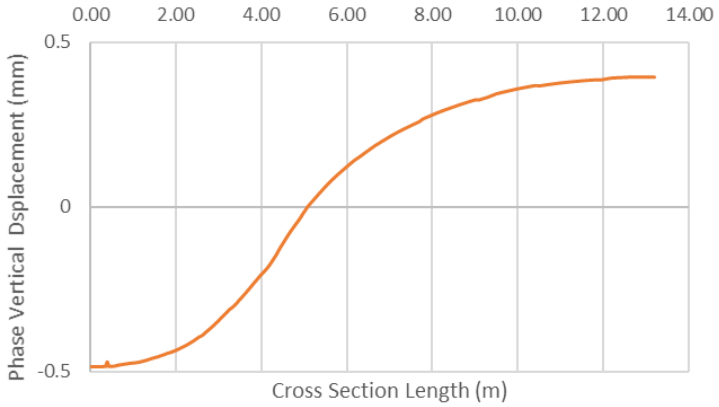

12: *Vertical displacements at crest dam along the line cross section E–E* (construction jet pile 1, 3, 5)

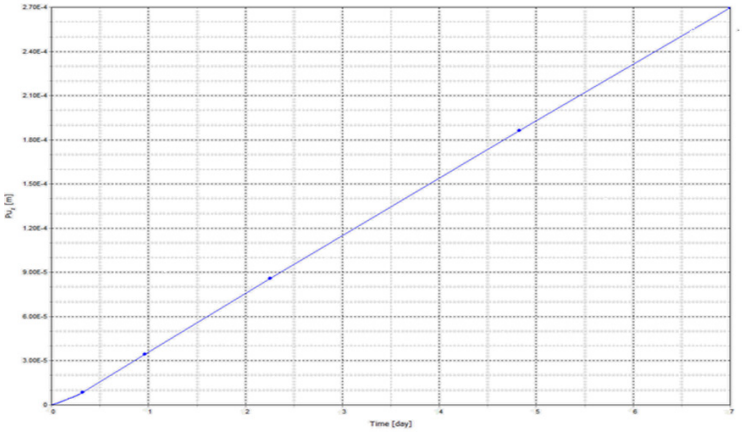

13: *Variation of total displacement with loading time*

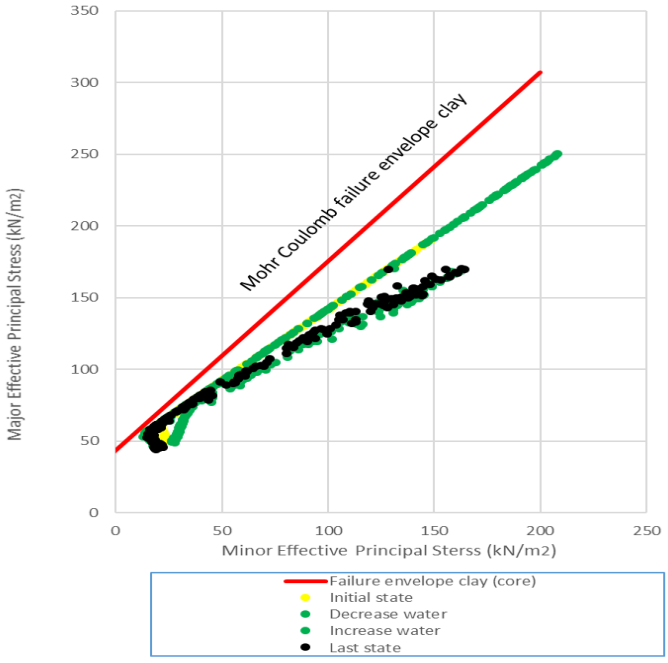

14: *The investigation of the failure for grouting system in the core*

CONCLUSION

It is quite difficult to model without specified material properties, so it should be input some reasonable values. In this study, the soil is assumed to behave as simple linear elastic, perfectly plastic isotropic materials with a Mohr-Coulomb failure criterion. The numerical investigation is conducted using Plaxis software which is based on the Finite Element Method (FEM), and the results are compared to the measured data performed by TBD company. The main findings in this study can be summarized as follows:

i) The jet pile construction is analysed by the presented 3D analysis considering the influence of pore water pressure.
ii) The horizontal displacement in connection zone during the construction stages reaches high value in step of decrease water during the reconstruction stages due to influence of water load and pore water pressure variation.
iii) The failure of the core does not occur for the connection system and no probability of hydraulic fracture occurrence in the connection zone.
iv) Good matching between the experimental and numerical results has been obtained using Plaxis
v) The applied element method is a reliable tool for processes of installing jet pile and excavating soil stages.
vi) Numerical evaluation using FEM analysis was successfully carried out to investigate the effects of installing jet piles on the surrounding soil.

LIST OF SYMBOLS

σ_x, σ_y, σ_z	Normal stress in direction (x, y, z)	[kN/m^2]
σ'_1, σ'_3	Major and minor effective principal stress	[kN/m^2]
τ_{xy}, τ_{yz}, τ_{zx}	Shear stress in direction (x, y, z)	[kN/m^2]
ε_x, ε_y, ε_z	Normal strain direction (x, y, z)	[-]
γ_{xy}, γ_{yz}, γ_{zx}	Shear strain in direction (x, y, z)	[-]
u, v, w	Displacement in direction (x, y, z)	[m]
p_w	Pore water pressure	[kN/m^2]
$H_1(t)$, $H_2(t)$	Piezometric head in boundaries borders	[m]
$h_{p,0}$	Initial piezometric head	[m]
H_0	Specified piezometric head in the reservoir	[m]
σ'_v	Vertical effective stress	[kN/m^2]
σ'_h	Horizontal effective stress	[kN/m^2]
K'_0	Coefficient for lateral earth pressure	[-]
F_x, F_y, F_z	Body forces per unit volume in direction (x, y, z)	[kN/m^3]
G	Shear modulus	[kN/m^2]
E	Elastic modulus	[kN/m^2]
ν	Poisson ratio	[-]
k_x, k_y, k_z	Coefficient of permeability of soil in direction (x, y, z)	[m/day]
n_i	Normal vector in directions	[-]
t	Time	[day]
m	Water storage	[m1-]
φ	Friction angle	[°]
c	Cohesion	[kN/m^2]
ψ	Dilatancy angle	[°]
σ'_N	Effective normal stress	[kN/m^2]
φ'	Effective angle of internal friction	[°]
ć	Effective cohesion	[kN/m^2]

REFERENCES

BRINKGREVE, R. B. J., ENGIN, E. and SWOLFS, W. M. 2017. PLAXIS 3D Anniversary edition, full manual. *Plaxis*. [Online]. Available at: https://www.plaxis.com/support/manuals/plaxis-3d-manuals [Accessed: 2017, May 25].

CROCE, P. and GIUSEPPE, M. 2007. Design of jet-grouting cut-offs. *Proceedings of the Institution of Civil Engineers Ground Improvement*, 11(1): 11–19.

FANG, S.Y., LIAO, J. J. and SZE, C, S. 1994. An empirical strength criterion for jet grouted soilcrete. *Engineering Geology*, 37(3): 285–293.

GALAVI, V. 2010. *Groundwater flow, fully coupled flow deformation and undrained analyses in PLAXIS 2D and 3D.* Technical report. Plaxis BV 2010, research department. [Online]. Available at: http://kb.plaxis.nl/publications/groundwater-flow-fully-coupled-flow-deformation-and-undrained-analyses-plaxis-2d-and-3d [Accessed: 2015, May 25].

HODÁK, J. 2014. VD Karolinka - (Karolinka Dam-Dam safety supervision during diaphragm wall construction). In: *Proceeding of the XXXIV. conference Priehradné dni 2014 conference*. Košice, SR: Slovenský vodohospodársky podnik, š.p. Odštepný závod Košice.

LABUZ, J. F. and ZANG, A., 2012. Mohr–Coulomb Failure Criterion. *Rock Mechanics and Rock Engineering*, 45(6): 975–979.

MICHAEL, R., THOMASH, K. and AGNEL, G. 2015. Seepage management control for a dam rehabilitation project using deep cut off wall construction and jet grouting. In: *Proceedings of the CDA 2015 Annual1Conference*.1Mississauga, ON, Canada. Available at: http://www.klohn.com/wpcontent/uploads/2016/01/150808_CDA-2015-Paper-Morrison-Dam-Submitted-ID1036.pdf [Accessed: 2015, October 5].

NIKBAKHTAN, B., AGHABABAEI, H. and POURRAHIMIAN, Y. 2007.1The effects of jet grouting on slope stability at Shahriar dam, Iran. In: *Proceedings of the 1st Canada-US Rock Mechanics Symposium.* 27–31 May, Vancouver, Canada. Available1at: https://www.researchgate.net/publication/280293011 [Accessed: 2017, October 25].

SCHWEIGER, H., GENS, A., WEI, S. L., CHEUK, J. and CHEANG, W. 2012. *PLAXIS Advanced course on computational geotechnics*. Hong Kong.

TAZAWA, E. and MIYAZAWA, S. 1997. Influence of constituents and composition on autogenous shrinkage of cementitious materials. *Magazine of Concrete Research*, 49(178): 15-22.

XANTHAKOS, P. P., ABRAMSON, L. W. AND BRUCE D. A. 1994. *Ground control and improvement*. 1st Edition. Wiley.

Contact information

Somia Bredy: bredy.s@fce.vutbr.cz
Jan Jandora: jandora.j@fce.vutbr.cz